Biochimica et Biophysica Acta 1837 (2014) 335–344

Contents lists available at ScienceDirect

Biochimica et Biophysica Acta

journal homepage: www.elsevier.com/locate/bbabio

Pre-diabetes alters testicular PGC1-α/SIRT3 axis modulating mitochondrial bioenergetics and oxidative stress

Luís Rato [a,b], Ana I. Duarte [b,c], Gonçalo D. Tomás [a], Maria S. Santos [b,d], Paula I. Moreira [b,e], Sílvia Socorro [a], José E. Cavaco [a], Marco G. Alves [a], Pedro F. Oliveira [a,*]

[a] CICS-UBI–Health Sciences Research Centre, University of Beira Interior, 6201-506 Covilhã, Portugal
[b] CNC—Center for Neuroscience and Cell Biology, University of Coimbra, 3004-517 Coimbra, Portugal
[c] Institute for Interdisciplinary Research (IIIUC), University of Coimbra, 3030-789 Coimbra, Portugal
[d] Life Sciences Department, Faculty of Sciences and Technology, University of Coimbra, 3004-517 Coimbra, Portugal
[e] Laboratory of Physiology, Faculty of Medicine, University of Coimbra, 3004-504 Coimbra, Portugal

ARTICLE INFO

Article history:
Received 24 September 2013
Received in revised form 10 December 2013
Accepted 12 December 2013
Available online 20 December 2013

Keywords:
High-energy diet
Mitochondria
PGC-1α/Sirt3 axis
Pre-diabetes
Testicular bioenergetics

ABSTRACT

Pre-diabetes, a risk factor for type 2 diabetes development, leads to metabolic changes at testicular level. Peroxisome proliferator-activated receptor γ coactivator 1 α (PGC-1α) and Sirtuin 3 (Sirt3) are pivotal in mitochondrial function. We hypothesized that pre-diabetes disrupts testicular PGC-1α/Sirt3 axis, compromising testicular mitochondrial function. Using a high-energy-diet induced pre-diabetic rat model, we evaluated testicular levels of PGC-1α and its downstream targets, nuclear respiratory factors 1 (NRF-1) and 2 (NRF-2), mitochondrial transcription factor A (TFAM) and Sirt3. We also assessed mitochondrial DNA (mtDNA) content, mitochondrial function, energy levels and oxidative stress parameters. Protein levels were quantified by Western Blot, mtDNA content was determined by qPCR. Mitochondrial complex activity and oxidative stress parameters were spectrophotometrically evaluated. Adenine nucleotide levels, adenosine and its metabolites (inosine and hypoxanthine) were determined by reverse-phase HPLC.

Pre-diabetic rats showed increased blood glucose levels and impaired glucose tolerance. Both testicular PGC-1α and Sirt3 levels were decreased. NRF-1, NRF-2 and TFAM were not altered. Testicular mtDNA content was decreased. Mitochondrial complex I activity was increased, whereas mitochondrial complex III activity was decreased. Adenylate energy charge was decreased in pre-diabetic rats, as were ATP and ADP levels. Conversely, AMP levels were increased, evidencing a decreased ATP/AMP ratio. Concerning to oxidative stress pre-diabetes decreased testicular antioxidant capacity and increased lipid and protein oxidation. In sum, pre-diabetes compromises testicular mitochondrial function by repressing PGC-1α/Sirt3 axis and mtDNA copy number, declining respiratory capacity and increasing oxidative stress. This study gives new insights into overall testicular bioenergetics at this prodromal stage of disease.

1. Introduction

Pre-diabetes is a major risk factor for the development of type 2 diabetes mellitus (T2DM) and is accompanied by elevated blood glucose levels, although not sufficient to meet the criteria for established diabetes [1]. It is characterized by impaired fasting glucose (IFG) and/or impaired glucose tolerance (IGT), and its prevalence is increasing among young people [1]. Every year, about 5–10% of the individuals with pre-diabetes become diabetic [2], and population habits may increase these rates. Moreover, in developed societies, the decrease of fertility rates has been associated with the increased incidence of diabetes mellitus (DM) [3]. Indeed, the effect of DM on male fertility has emerged as an alarming issue, further exacerbated by the increasing number of children and adolescents with T2DM [4], which present a transition time between pre-diabetes and T2DM even shorter than adult individuals [5,6].

Abbreviations: ADP, adenosine diphosphate; AEC, adenylate energy charge; AMP, adenosine monophosphate; ATP, adenosine triphosphate; AUC_g, area under the curve for glucose tolerance test; BSA, bovine serum albumin; DCPIP, dichlorophenolindophenol; DM, diabetes mellitus; DNPH, 2,4-dinitrophenylhydrazine; ETC, electron transport chain; FRAP, ferric reducing antioxidant power; GLUT1, glucose transporter 1; HED, high-energy diet; IFG, impaired fasting glucose; IGT, impaired glucose tolerance; mtDNA, mitochondrial DNA; mtND1 gene, mitochondrial ND1 gene; NRF-1, nuclear respiratory factor 1; NRF-2, nuclear respiratory factor 2; OXPHOS, oxidative phosphorylation system; PGC-1α, peroxisome proliferators-activated receptor γ coactivator 1 α; ROS, reactive oxygen species; Sirt3, Sirtuin 3; STZ, streptozotocin; T2DM, type 2 diabetes mellitus; TBA, thiobarbituric acid; TBARS, thiobarbituric acid reactive species; TFAM, mitochondrial transcription factor A; TPTZ, 2,4,6-tripyridyl-s-triazine; β2MG, beta-2-microglobulin gene

* Corresponding author. Tel.: +351 275 329077.
E-mail address: pfobox@gmail.com (P.F. Oliveira).

0005-2728/$ – see front matter © 2013 Elsevier B.V. All rights reserved.
http://dx.doi.org/10.1016/j.bbabio.2013.12.008

"Western" lifestyle habits, such as overeating and sedentary life, have contributed to the increased infertility and subfertility prevalence associated to DM [7,8]. Emerging evidence supports that dietary lifestyle affects male fertility. For instance, Attaman and collaborators [9] showed a moderate association between dietary fats and semen quality. Similarly, Jensen and collaborators [10] also reported that high fat intake affects sperm count and sperm concentration of Danish men. These results are also in line with data from animal studies [11,12], supporting that saturated fatty acid intake is deleterious for male reproductive performance. The hyperglycemic state resultant from diabetic conditions contributes for an impaired reproductive function [13–15]. Recently our team reported that diet-induced pre-diabetes alters testicular metabolism, compromising sperm quality parameters, with a marked increase in abnormal sperm morphology [14]. However, little is known on the molecular mechanisms underlying male reproductive dysfunction in the diet-induced pre-diabetic state. Mitochondria are the best-known cellular powerhouses and form an interconnected network that is integrated with other cellular compartments. This organelle is of great importance, since it is essential for functional sperm, and thus, to ensure a normal spermatogenic event. Peroxisome proliferator-activated receptor gamma coactivator 1-α (PGC-1α) is a member of a small family of transcriptional regulators which controls the expression of genes involved in energy homeostasis, mitochondrial biogenesis, fatty acid oxidation and glucose metabolism [16,17]. PGC-1α stimulates the expression of transcriptional regulators, the nuclear respiratory factors 1 and 2 (NRF-1 and NRF-2) that act on the nuclear genes coding for subunits of the oxidative phosphorylation (OXPHOS) system. Mitochondrial transcription factor A (TFAM) is a downstream target of both NRF-1 and NRF-2 that activates the transcription via sequence specific binding in the mitochondrial promoters [18]. TFAM gene presents consensus-binding sites for both NRF-1 and NRF-2 providing a unique mechanism for the cell integrates the expression of nuclear DNA-encoded proteins with the transcription of genes encoded by mtDNA [18]. Undoubtedly, PGC-1α is pivotal for mitochondrial function, as well as for the expression of key mitochondrial proteins, such as Sirtuin 3 (Sirt3) [16]. Sirt3 is a member of sirtuins family of NAD^+-dependent class III histone deacetylases and/or protein ADP-ribosyltransferases that mediate adaptive responses to a variety of stresses [19]. Among the seven members of the sirtuins family, Sirt3 is of particular interest concerning the mitochondrial function, as this protein is preferentially allocated in this organelle [19]. Similarly to PGC-1α, Sirt3 promotes metabolic reprogramming by activating enzymes involved in mitochondrial fuel catabolism [20]. Sirt3 modulates mitochondrial energy homeostasis by regulating ATP generation from OXPHOS [21] and interacts with the enzymatic complexes of the electron transport chain (ETC), resulting in increased activity of complexes and contributing to an efficient electron flow through ETC [22]. Interestingly, PGC-1α and Sirt3 act synergistically to maintain mitochondrial biogenesis, functional OXPHOS and an active ROS defense system [16]. It has been reported that PGC-1α and Sirt3 are downregulated in the skeletal muscle of high-fat fed rats [23], and the lack of PGC-1α and/or Sirt3 favors oxidative stress, due to an imbalance between ROS and antioxidant defenses [24]. ROS overproduction damages mtDNA, which compromises the expression of OXPHOS genes resulting in a mitochondrial respiratory dysfunction.

Herein we hypothesize that PGC-1α/Sirt3 axis could play a major role in testicular bioenergetic metabolism and ultimately in spermatogenesis of pre-diabetic individuals. Available information concerning mitochondrial testicular bioenergetics in DM is often associated with more advanced or severe stages of the disease [25] and there are no studies at the initial stages of this pathology. Thus, using a high-energy diet (HED) male rat model that develops a pre-diabetic state, we aimed to evaluate the effects of pre-diabetes on testicular expression of PGC-1α and its downstream targets Sirt3, NRF-1, NRF-2, TFAM and on testicular ETC function. We also evaluated the effects on testicular mtDNA integrity, testicular adenylate energy charge (AEC) and on particular oxidative stress parameters, such as antioxidant capacity, lipid peroxidation and carbonyl content.

2. Material and methods

2.1. Chemicals

DNeasy® Blood & Tissue kit (Cat. Nº 69504, Qiagen, Hilden, Germany), Maxima SYBR Green qPCR Master Mix (Fermentas, Vilnius, Lithuania), DCPIP (D1878, Sigma-Aldrich, St Louis, MO, USA), NADH (N6005, Sigma-Aldrich, St Louis, MO, USA); Coenzyme Q1 (C7956, Sigma-Aldrich, St Louis, MO, USA), Decylubiquinone (D7911, Sigma-Aldrich, St Louis, MO, USA), cytochrome c (C30398, Sigma-Aldrich, St Louis, MO, USA), n-Dodecyl β-D-maltoside (D4641, Sigma-Aldrich, St Louis, MO, USA), protease cocktail inhibitor (P8340, Sigma-Aldrich, St Louis, MO, USA), anti-Sirt3 polyclonal antibody was purchased at Cell Signaling (Beverly, USA), anti-PGC1-α, anti-TFAM and anti-NRF-1 were purchased at Santa Cruz Biotechnology, Inc. (USA), and anti-NRF-2 was purchased at Abcam (Cambridge, UK). ECF™ substrate was purchased at GE, Healthcare (Orsay, France). All other chemicals were purchased at Sigma-Aldrich (St Louis, MO, USA).

2.2. Animals

In the present study, we used 12 two-month-old male Wistar rats (Charles River Laboratories, Barcelona, Spain). The animals were housed in our accredited animal colony (Health Sciences Research Centre, University of Beira Interior) and maintained on ad libitum food and water, at constant temperature (20 ± 2 °C) and with a 12-hour cycle of artificial lighting. All animal experiments were performed according to the "Guide for the Care and Use of Laboratory Animals" published by the US National Institutes of Health (NIH Publication No. 85–23, revised 1996) and the European rules for the care and handling of laboratory animals (Directive 86/609/EEC).

2.3. Animal model and experimental design

Rats were randomly divided (6 per group) in control and high-energy diet (HED) groups. In control group, animals were fed with a standard chow diet (4RF21 certificate, Mucedola, Italy), while HED group received an additional high-energy emulsion, as described elsewhere [14,26–28]. Briefly, in the first 5 days of treatment, animals were given progressively 1 to 5 mL of emulsion by gavage consisting of 20 g lard oil, 1 g thyreostat, 5 g cholesterol, 1 g sodium glutamate, 10 g sucrose, 20 mL Tween 80, 30 mL propylene glycol, prepared in a final volume of 100 mL by adding distilled water. Then, they were administrated daily with 5 mL of the emulsion until reaching one month of treatment. Water was administered to the respective control group.

Animal's blood glucose levels were monitored every 6 days. After treatment, animals were killed by cervical dislocation. Blood was collected by cardiac puncture to non-heparinized tubes. Testicles were removed, weighed and stored at −80 °C. Non-fasting glycaemia was determined using a glucometer (One Touch Ultra Lifescan-Johnson, Milpitas, CA, USA) and insulin levels were determined using commercial rat EIA kits (Mercodia, Uppsala, Sweden), according to the manufacturer's instructions.

At 3 months of age, animals were submitted to a glucose tolerance test, as described by Rato and collaborators [14]. Briefly, 14–18 h before the test, food was removed and animals were kept in fasting. An intraperitoneal injection with 6 mL glucose 30% (w/v) per kg of body weight was given to each animal. Blood glucose levels were measured at 30, 60, 90 and 120 min after glucose loading. The area under the curve for glucose tolerance (AUC_g) was calculated using trapezoidal rule.

2.4. Western Blot

Western Blot procedure was performed as previously described by Simões and collaborators [29]. The resulting membranes were incubated with rabbit anti-PGC-1α (1:1000, sc-13067, Santa Cruz Biotechnology), rabbit anti-NRF-1 (1:1000, sc-33771, Santa Cruz Biotechnology), goat anti-TFAM (1:500, sc-23588, Santa Cruz Biotechnology), rabbit anti-NRF-2 (1:1000, ab31163, Abcam), rabbit anti-Sirt3 (1:1000, C73E3, Cell Signaling Technology Inc.) or mouse anti-tubulin (1:5000, T9026, Sigma-Aldrich) was used as protein loading control for testicular tissue. The immuno-reactive proteins were detected separately with goat anti-rabbit IgG-AP (1:5000, Sc2007, Santa Cruz Biotechnology) or goat anti-mouse IgG-AP (1:5000, Sc2008, Santa Cruz Biotechnology) or rabbit anti-goat IgG-AP (1:20000, A4187 Sigma-Aldrich). Membranes were reacted with ECF™ detection system (GE, Healthcare). The densities from each band were obtained using the Quantity One Software (Bio-Rad, Hemel Hempstead, UK), divided by the respective tubulin band density and then normalized against the respective control.

2.5. mtDNA relative copy number

Total DNA was extracted from tissues using the DNeasy® Blood & Tissue kit, according to the manufacturer's instructions.

mtDNA relative copy number of the experimental groups was determined by qPCR analysis, as described by Wai and collaborators [30] with slight modifications. Relative quantification of mtDNA levels was determined by the ratio between the mitochondrial ND1 (mtND1) gene and the single-copy, nuclear-encoded beta-2-microglobulin (β2MG) gene. Reactions were carried out in an iQ5 system (Bio-Rad, Richmond, CA, USA), and the efficiency of the reactions was determined for the selected primers using serial dilutions of DNA samples. The specificity of the amplicons was determined by melting curve analysis. The reaction mixture consisted of Maxima SYBR Green qPCR Master Mix, 200 nM of each sense and antisense primers (see Table 1 for details) and 20 ng of DNA. Each reaction was run in triplicate to calculate relative mtDNA copy number. Ct values of all samples were within the linear range. Ct value differences were used to quantify mtDNA copy number relative to the β2MG gene with the following equation: Relative copy number $= 2^{-\Delta\Delta Ct}$, where ΔCt is $Ct_{\beta 2MG} - Ct_{ND1}$.

2.6. Citrate synthase activity

Citrate synthase activity was determined by modification of a method previously described by Core and collaborators [31]. Briefly, testicular tissue was homogenized using lysis buffer (250 mM Sucrose, 5 mM HEPES, pH 7.4). Protein concentration was determined by the Bradford micro assay using BSA (bovine serum albumin) as a standard. 25 μg of tissue homogenate was incubated at 37 °C in a reaction buffer containing 100 mM Tris pH 8.0 plus 200 μM Acetyl-CoA, 200 μM 5,5′-dithiobis-2-nitrobenzoic acid. Enzymatic activity was determined in a VICTOR X3 plate reader (Perkin-Elmer Cetus, Norwalk, CO, USA), at 37 °C, by following the increase in absorbance (412 nm) upon addition of 100 μM freshly-prepared oxaloacetate. Enzyme activity was calculated through the mean of the slopes of duplicates obtained during the linear phase. Citrate synthase-specific activity was calculated by subtracting the basal activity in the presence of 0.1% Triton-X100. A molar extinction coefficient of $\varepsilon_{412} = 13.6\ mM^{-1}\cdot cm^{-1}$ and normalization to protein amount were applied. Enzyme activity was expressed as nmol of oxaloacetate $min^{-1}\cdot mg\ protein^{-1}$.

Table 1
Oligonucleotides and cycling conditions for qPCR amplification of ND1 and β-2-microglobulin.

Gene	Sequence (5′–3′)	AT (°C)	Amplicon size (bp)
ND1	Sense: GAG CCC TAC GAG CCG TTG CC Antisense: GCG AATG GTC CTG CGG CGT A	58	271
β2MG	Sense: GCG TGG GAG GAG CAT CAG GG Antisense: CTCATCACCACCCCGGGGACT	58	264

Abbreviations: AT — annealing temperature.

2.7. NADH-ubiquinone oxidoreductase activity

Complex I activity was determined by modification of a method previously described by Long and collaborators [32]. Briefly, 30 μg of tissue homogenate (obtained as previously described) was diluted in reaction buffer containing 25 mM KH_2PO_4 pH 7.5, 5 mM $MgCl_2$, 300 μM KCN, 4 μM antimycin A, 3 $mg\cdot mL^{-1}$ BSA, 60 μM coenzyme Q1, 160 μM 2,6-dichlorophenolindophenol (DCPIP). Complex I activity was measured at 37 ºC, in a VICTOR X3 plate reader, by following the decrease in absorbance (600 nm) of DCPIP upon addition of 100 μM freshly-prepared NADH. Enzyme activity was calculated through the mean of slopes of duplicates, obtained during the linear phase. Mitochondrial complex I specific activity was determined as the difference between basal activity in the absence or presence of 10 μM rotenone (specific inhibitor of complex I). A molar extinction coefficient of $\varepsilon_{600} = 19.1\ mM^{-1}.cm^{-1}$ and normalization to protein amount were applied. Complex I activity was expressed as nmol DCPIP $min^{-1}\cdot mg\ protein^{-1}$.

2.8. Succinate-cytochrome c reductase activity

Complex II/III activity was determined by modification of a method previously described by Tisdale [33]. Briefly, 100 μg of tissue homogenate (obtained as described above) was preincubated for 5 min, at 37 °C, in 200 μL of phosphate buffer (166 mM KH_2PO_4/K_2HPO_4, pH 7.4) supplemented with 100 mM KCN and 500 mM sodium succinate. The reaction was initiated by the addition of 120 μL of phosphate buffer supplemented with 2 mM oxidized cytochrome c (cyt c_{ox}) plus 15 mM EDTA-dipotassium. Enzyme activity was calculated through the mean of slopes of duplicates, obtained during the linear phase. Complex II/III activity was measured by following the reduction of cyt c_{ox} (increased absorbance at 550 nm), using a VICTOR X3 plate reader. Mitochondrial complex II/III specific activity was determined as the difference between basal activity in the absence or presence of 4 mM antimycin A (specific inhibitor of complex III). A molar extinction coefficient of $\varepsilon_{550} = 19.1\ mM^{-1}\cdot cm^{-1}$ and normalization to protein amount were applied. Results were express as nmol cyt c_{ox} $min^{-1}\cdot mg\ protein^{-1}$.

2.9. Cytochrome c reductase activity

Complex III activity was determined by modification of a method previously described Luo and collaborators [34]. Briefly, 100 μg of tissue homogenate (obtained as previously referred) was incubated in reaction buffer containing 25 mM KH_2PO_4 pH 7.5, 4 uM rotenone, 0.025% Tween-20, 100 μM fresh decylubiquinone solution at 37 °C. Enzymatic activity was followed by an increase in absorbance of cyt c_{ox} at 550 nm, upon addition of 75 μM cyt c_{ox} in a VICTOR X3 plate reader. Enzyme activity was calculated through the mean of slopes of duplicates, obtained during the linear phase. Mitochondrial complex III specific activity was determined as the difference between basal activity in the absence or presence of 2.5 mM antimycin A (complex III specific inhibitor). A molar extinction coefficient of $\varepsilon_{550} = 19.1\ mM^{-1}\cdot cm^{-1}$ and normalization to protein amount were applied to express the activity as nmol cyt c_{ox} $min^{-1}\cdot mg\ protein^{-1}$.

2.10. Cytochrome c oxidase activity

Complex IV activity was determined by modification of a method previously described by Brautigan and collaborators [35]. Briefly, 25 μg of tissue homogenate (obtained as previously described) was incubated at 37 °C, in reaction buffer containing 50 mM KH_2PO_4 pH 7.0, 4 μM antimycin A, 0.05% n-dodecyl-β-D-maltoside. Enzymatic activity was

followed by a decrease in absorbance of reduced cytochrome c (cyt c_{red}) at 550 nm, upon addition of 57 μM freshly-prepared cyt c_{red} in a VICTOR X3 plate reader. Enzyme activity was calculated through the mean of slopes of duplicates, obtained during the linear phase. Mitochondrial complex IV specific activity was determined as the difference between basal activity in the absence or presence of 10 mM of KCN (complex IV specific inhibitor). A molar extinction coefficient of $\varepsilon_{550} = 19.1\ mM^{-1}\cdot cm^{-1}$ and normalization to protein amount were applied. Activity was expressed as nmol cyt c_{red} $min^{-1}\cdot mg\ protein^{-1}$.

2.11. Analysis of adenine nucleotides and adenosine metabolites

Adenine nucleotide and adenosine metabolite levels were measured according to previously described methods by Rego and collaborators [36]. Briefly, testicular tissue was homogenized in lysis buffer (250 mM sucrose, 20 mM HEPES, 10 mM KCl, 1.5 mM $MgCl_2$, 1 mM EDTA, 1 mM EGTA, pH 7.4) supplemented with 1% protease inhibitor cocktail, 1 mM DTT and 1 mM PMSF and centrifuged at 14,000 ×*g*, for 2 min at (0–4 °C). After neutralization with 3 M KOH in 1.5 M Tris, samples were centrifuged at 14,000 ×*g* for 2 min (0–4 °C). The resulting supernatants were used to determine protein concentration by the Bradford micro assay using BSA as a standard. The supernatant was assayed for ATP, ADP, AMP, adenosine and its metabolites (inosine and hypoxanthine), by separation in a reverse-phase high-performance liquid chromatography (HPLC), as described by Stocchi and collaborators [37]. The chromatographic apparatus used was a Beckman-System Gold (Beckman Instruments, Fullerton, USA), consisting of a 126 Binary Pump Model and 166 Variable UV detector, controlled by a computer. The detection wavelength was 254 nm, and the column used was a LiChrospher 100 RP-18 (5 μm) from Merck (Darmstadt, Germany). An isocratic elution with 100 mmol/L phosphate buffer (KH_2PO_4; pH 6.5) and 1.0% methanol was performed with a flow rate of 1 mL/min. The required time for each analysis was 6 min. Peak identity was determined by the retention time compared with standards. The amounts of nucleotides and metabolites were determined by a concentration standard curve. Testicular AEC was determined according to the formula: ATP + 0.5 × ADP /(ATP + ADP + AMP).

2.12. Ferric reducing antioxidant power assay

The ferric reducing antioxidant power (FRAP) of the media samples was performed according to the colorimetric method described by Benzie and Strain [38]. Briefly, testicular tissue was homogenized in phosphate buffer (pH 7.4). Protein concentration was determined by the Bradford micro assay using BSA as a standard. Working FRAP reagent was prepared by mixing acetate buffer (300 mM, pH 3.6), 2,4,6-Tripyridyl-s-Triazine (TPTZ) (10 mM in 40 mM HCl) and $FeCl_3$ (20 mM) in a 10:1:1 ratio (v:v:v). 180 μL of this reagent was mixed with 10 μg of tissue homogenate. The reduction of the Fe^{3+}-TPTZ complex to a colored Fe^{2+}-TPTZ complex by the samples was monitored immediately after adding the sample and 40 min later, by measuring the absorbance at 595 nm using an Anthos 2010 microplate reader (Biochrom, Berlin, Germany). Antioxidant potential of the samples was determined against standards of ascorbic acid, which were processed in the same manner as the samples. Absorbance results were corrected by using a blank, with H_2O instead of sample.

2.13. Thiobarbituric acid reactive species assay

Thiobarbituric acid reactive species (TBARS) are formed as a byproduct of lipid peroxidation, which can be detected by the TBARS assay using thiobarbituric acid (TBA) as a reagent. This peroxidation reaction produces malonaldehyde (MDA) that reacts with TBA in conditions of high temperature and low pH, generating a pink colored complex, which absorbs at 532 nm [39]. TBARS assay was carried out by the method described by Iqbal and collaborators [40] with slight modifications. Testicular tissue was homogenized in phosphate buffer (pH 7.4). Protein concentration was determined by the Bradford micro assay using BSA as standard. Briefly, 20 μg of tissue homogenate, 0.01 mL Tris–HCl buffer (150 mM, pH 7.1), 0.01 mL ferrous sulphate (1.0 mM), 0.01 mL ascorbic acid (1.5 mM) and 0.06 mL H_2O were mixed in a reaction tube. This mixture was incubated at 37 °C for 15 min. The reaction was stopped by addition of 0.1 mL of trichloroacetic acid (10% w/v). Subsequently, 0.2 mL of TBA (0.375% w/v) were added and all samples were incubated for 15 min at 100 °C. Finally, samples were centrifuged at 1000 ×*g* for 10 min. The amount of MDA formed in each sample was estimated by measuring optical density at 532 nm using a UV–VIS spectrophotometer (Shimadzu, Kyoto, Japan) against a blank. The results were expressed as nmol of TBARS/mg protein.

2.14. Analysis of carbonyl groups

Protein carbonyl content is commonly used as a marker for protein oxidation. To evaluate protein carbonyl groups a Slot Blot was performed. First, samples were derivatized using 2,4-dinitrophenylhydrazine (DNPH) according to the method developed by Levine and collaborators [41]. Briefly, a volume containing 40 μg of lyophilized testicular tissue homogenized in phosphate buffer was mixed with the same volume of SDS 12% and centrifuged to minimize nucleic acid interference in the assay. The samples were then mixed with two volumes of DNPH 20 mM diluted in TFA 10% and incubated for 30 min in a dark environment. The reaction was stopped using 1.5 volumes of Tris 2 M diluted in β-mercaptoethanol. Samples were then diluted to a concentration of 0.001 μg/μL using phosphate buffer. A previously activated polyvinylidenedifluoride membrane was used in the Slot-Blot, which was performed in a Hybri-slot manifold system (Biometra, Germany). The membranes were then incubated for 90 min with a 5% non-fat milk solution. Afterwards, membranes were incubated overnight with rabbit anti-DNP antibody (1:5000 D9656; Sigma Aldrich). Samples were visualized using anti-rabbit IgG-AP. Membranes were then reacted with ECF™ substrate (GE, Healthcare) and read using a BioRad FX-Pro-plus (Bio-Rad, UK). Densities from each band were quantified using the BIO-PROFIL Bio-1D Software from Quantity One (VilberLourmat, Marne-la-Vallée, France).

2.15. Statistical analysis

The statistical significances of the differences between all experimental data were assessed by unpaired Student's t-test (GraphPad Software, San Diego, CA, USA). All experimental data are shown as mean ± SEM of the indicated number of independent experiments. $P < 0.05$ was considered significant.

3. Results

3.1. High-energy diet fed rats developed mild hyperglycemia, glucose intolerance and hypoinsulinemia

HED rodent model was developed as previously described by our team [14,42]. At the end of HED treatment, animals presented mild hyperglycemia (Fig. 1A). Moreover, HED rats had significantly increased (by ~57%) AUC_g values compared to control group (Fig. 1B), evidencing that HED rats developed significant glucose intolerance. These results suggested an insulin dysfunction status, so we measured fasting blood insulin levels and, as expected, insulin levels of HED rats were significantly decreased (by ~61%) when compared to control group (Fig. 1C). These characteristics, particularly glucose intolerance and mild-hyperglycaemia, indicated that HED animals developed a pre-diabetic state.

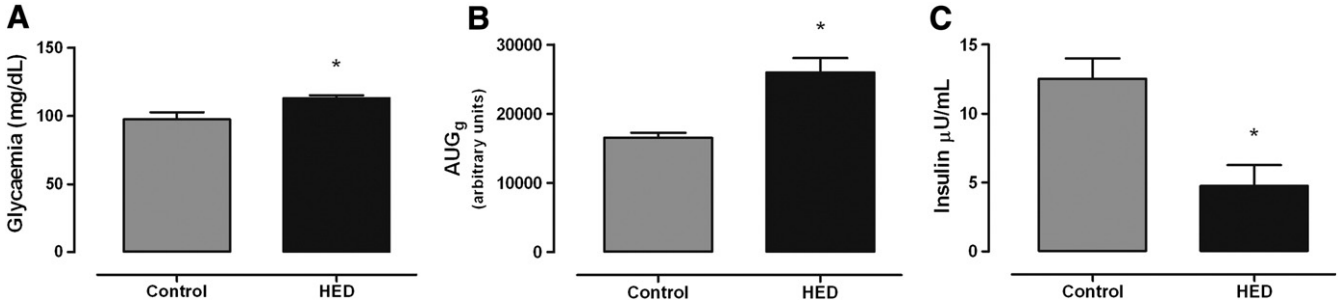

Fig. 1. A) Blood glucose levels of control group and HED group animals after 30 days of treatment. B) AUCg of the intraperitoneal glucose tolerance test performed in control group and HED group animals. C) Insulin levels of control group and HED group animals after 30 days of treatment. Results are presented as mean ± SEM of six independent experiments, corresponding to six animals/group. *$P < 0.05$ vs. control group. HED—high-energy diet. AUCg—area under the curve for glucose tolerance test.

3.2. Pre-diabetes compromises testicular mitochondrial biogenesis by decreasing PGC-1α protein levels

High-energy diets are known to downregulate PGC-1α protein levels [23], thus we evaluated the effects of pre-diabetes in testicular PGC-1α protein levels and we observed a 1.53-fold reduction in HED animals when compared to control group (Fig. 2; Panels A and B). As PGC-1α is considered the key regulator of mitochondrial biogenesis, the decreased levels of PGC-1α may compromise this cellular process, so we quantified the protein levels of its downstream targets: NRF-1, NRF-2 and TFAM. The obtained results showed no differences between groups for both nuclear transcriptors NRF-1 and NRF-2, as well as, the key activator of mitochondrial transcription and mtDNA replication, TFAM (Fig. 2; Panels A and B).

3.3. Pre-diabetes significantly decreased testicular levels of Sirtuin 3

In addition, since PGC-1α is crucial for the expression of Sirt3, we further quantified the protein levels of this mitochondrial deacetylase. Sirt3 is the most important deacetylase that modulates mitochondrial metabolism and oxidative stress [24]. Sirt3 protein levels were decreased by 2-fold in HED animals when compared to control group (Fig. 2; Panels A and B). The decreased levels of testicular Sirt3 may contribute to a compromised testicular mitochondrial function and increased oxidative stress, so we further assessed mitochondrial function and oxidative stress parameters.

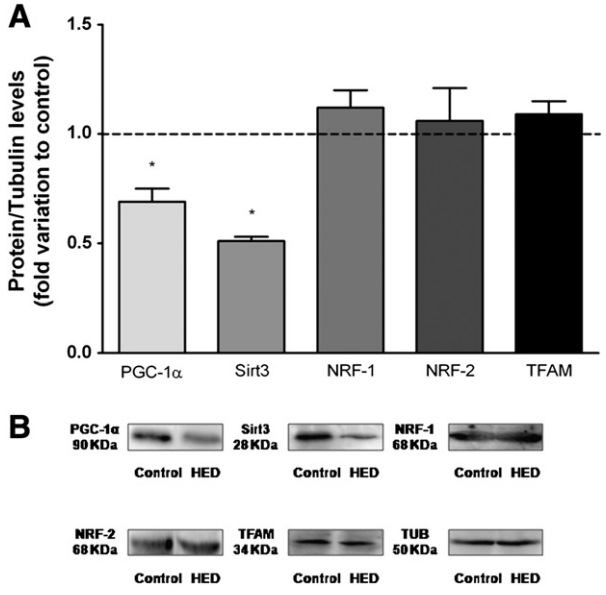

Fig. 2. Effect of high-energy diet (HED) on testicular PGC-1α, Sirt3, NRF-1, NRF-2 and TFAM protein (Part A) levels. Part B represents an illustrative Western Blot experiment. Results are presented as mean ± SEM of five independent experiments, corresponding to five animals/group and performed in triplicate. *$P < 0.05$ vs. control group.

3.4. Pre-diabetes significantly decreased testicular mtDNA copy number

mtDNA comprises genes encoding for polypeptides that constitute the multi-subunit enzyme complexes of the respiratory chain. Alterations in mtDNA content have been associated to disturbances in the activity of ETC [43]. Therefore, we determined the effects of HED on testicular tissue mtDNA content. We observed a 38.8% decrement in mtDNA content in HED rat testicles compared to control group (Fig. 3; Panel A). This suggests that mitochondrial respiratory function may be affected in these conditions. Thus, we determined ETC complexes activity in order to evaluate possible testicular mitochondrial bioenergetics alterations induced by pre-diabetes.

3.5. Mitochondrial complex I and complex III activities were altered in testicles of pre-diabetic rats

Mitochondrial function is highly dependent on the activities of several mitochondrial enzymes, such as citrate synthase and respiratory complexes I to IV. Citrate synthase activity is a marker for testicular mitochondrial content and integrity [31]. In this regard, we did not find significant differences in testicular tissue from animals of both groups (Fig. 3; Panel B).

We also evaluated the enzymatic activities of mitochondrial respiratory complexes I to IV (Fig. 3C–F). Despite no significant differences in both succinate cytochrome c reductase (complex II-III) and cytochrome c oxidase (complex IV) activities in testicular tissue from animals of both groups (Fig. 3D and F), NADH reductase (complex I) activity was increased by 79% in HED rat testicles compared to control (Fig. 3C). Testicular cytochrome c reductase (complex III) activity of HED rats was decreased from 448 ± 97 nmol/min (in control rats) to 236 ± 73 nmol/min (Fig. 3E).

3.6. Testicular adenylate energy charge was significantly decreased by pre-diabetes

Testicles are organs with high-energy demands and the AEC is often used to evaluate overall energetic status of cells and tissues [44,45]. Thus, we analyzed the HED effect in adenine nucleotides metabolism and in testicular AEC. ATP content was 39% lower in testicles of HED than in control rats (Fig. 4A). Likewise, ADP content in testicular tissue of HED rats showed a significant decrease (by 56%) when compared with control animals (Fig. 4B). Conversely, testicular AMP content was increased by 89% in HED rats (Fig. 4C). As a consequence of the lower levels of ATP and the significant increase in AMP content, lower ATP/AMP ratio in testicles of HED rats when compared with control animals (Fig. 4D) was detected.

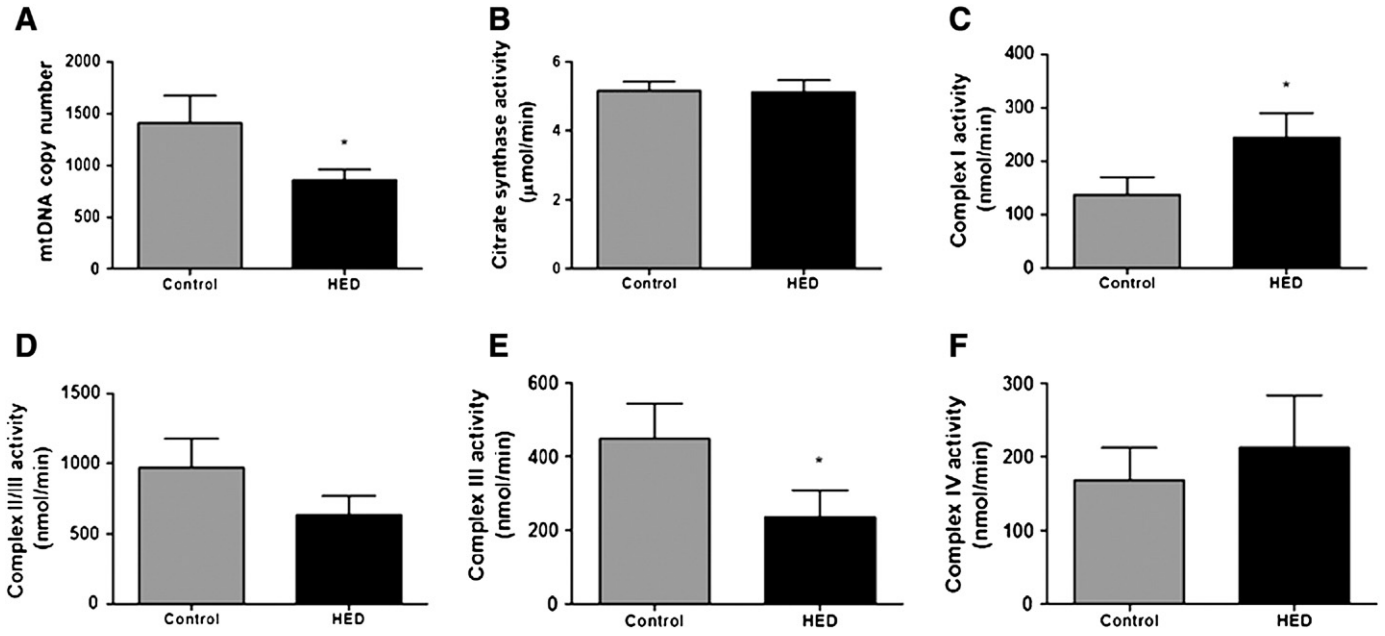

Fig. 3. A) Relative mtDNA copy number in control group and HED group. B) Citrate synthase activity; C) NADH reductase (Complex I) activity; D) succinate cytochrome c reductase (Complex II/III) activity; E) cytochrome c reductase (Complex III) activity; F) cytochrome c oxidase (Complex IV) activity. Results are presented as mean ± SEM of five independent experiments, corresponding to five animals/group and performed in triplicate. *$P < 0.05$ vs. control group.

As expected, the overall testicular AEC was 3.4-fold decreased in HED rats when compared to control animals (Fig. 4E). The lower testicular AEC level in HED rats points to low energy levels in testicular *milieu*, with a high accumulation of AMP.

3.7. Pre-diabetes alters testicular adenosine metabolites

The lower testicular ATP/AMP observed in HED rats leads us to hypothesize that ATP metabolism should be progressing to adenosine formation. In fact, the conversion of AMP to adenosine is a final common step in the catabolism of the adenine nucleotides [46]. Herewith, we did not observed significant differences on the testicular adenosine levels between animals from both groups (Table 2). Interestingly, we found that inosine content was decreased by 54% in testicles of HED rat compared with the animals from the control group (Table 2), while hypoxanthine content raised by 24% in HED animals compared to control animals (Table 2). These results suggest that pre-diabetes favors adenine nucleotides metabolism in which AMP is converted to adenosine subproducts, namely hypoxanthine, suggesting an oxidative state.

3.8. Pre-diabetes favors testicular oxidative environment

To evaluate the effects of pre-diabetes on testicular antioxidant capacity we utilized the FRAP assay. The FRAP assay measures the potential to reduce ferric (III) to ferrous (II) in a redox-linked colorimetric reaction that involves single electron transfer [38]. This reducing

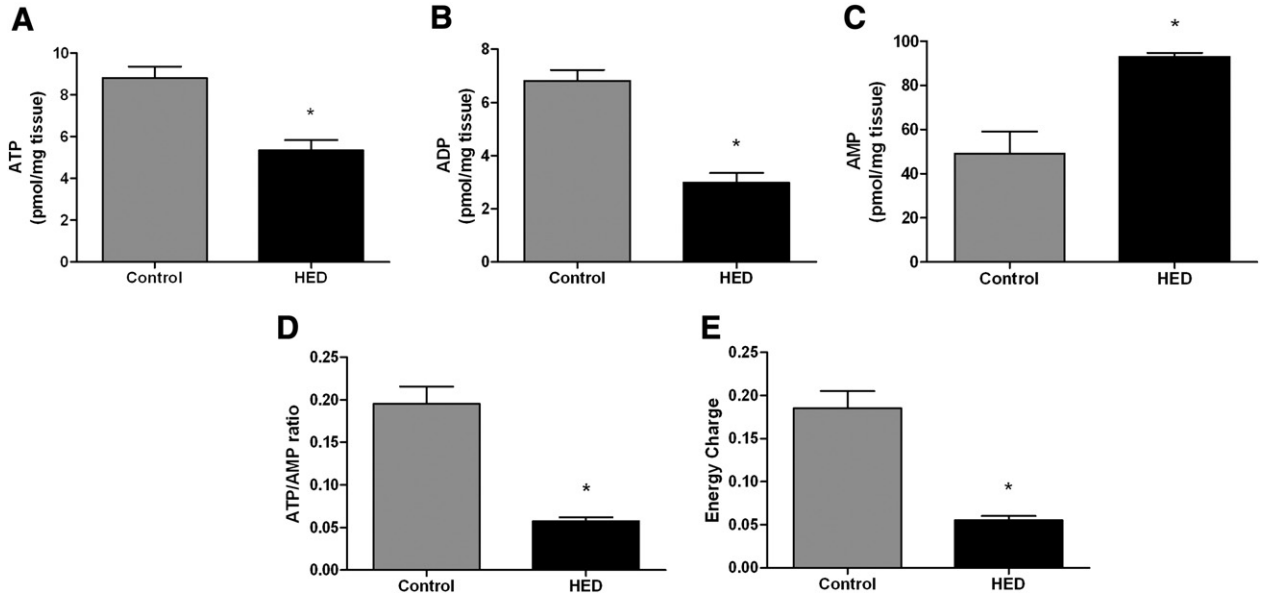

Fig. 4. Testicular adenine nucleotides levels in control group and HED group. A) ATP; B) ADP; C) AMP; D) ATP/AMP ratio; E) Testicular adenylate energy charge. Results are presented as mean ± SEM of five independent experiments, corresponding to five animals/group and performed in duplicate. *$P < 0.05$ vs. control group.

Table 2
Average values of the testicular adenosine metabolites measured in Control group and in HED group.

Adenosine metabolites	Control group	HED group
Adenosine (pmol/mg tissue)	7.34 ± 0.72	6.74 ± 0.26
Inosine (pmol/mg tissue)	49.89 ± 2.21	23.19 ± 4.88*
Hypoxanthine (pmol/mg tissue)	137.07 ± 3.17	170.97 ± 5.25*

HED: high-energy diet. Results are expressed as means ± SEM (n = 5 for each condition).
* Significantly different relative to control ($P < 0.05$).

power serves as a significant indicator of the potential antioxidant activity (FRAP value). The results showed that antioxidant capacity was decreased by 55% in testicles of HED animals when compared to control group (Fig. 5A). The decreased antioxidant capacity in HED rat testicles may favor a high testicular ROS activity.

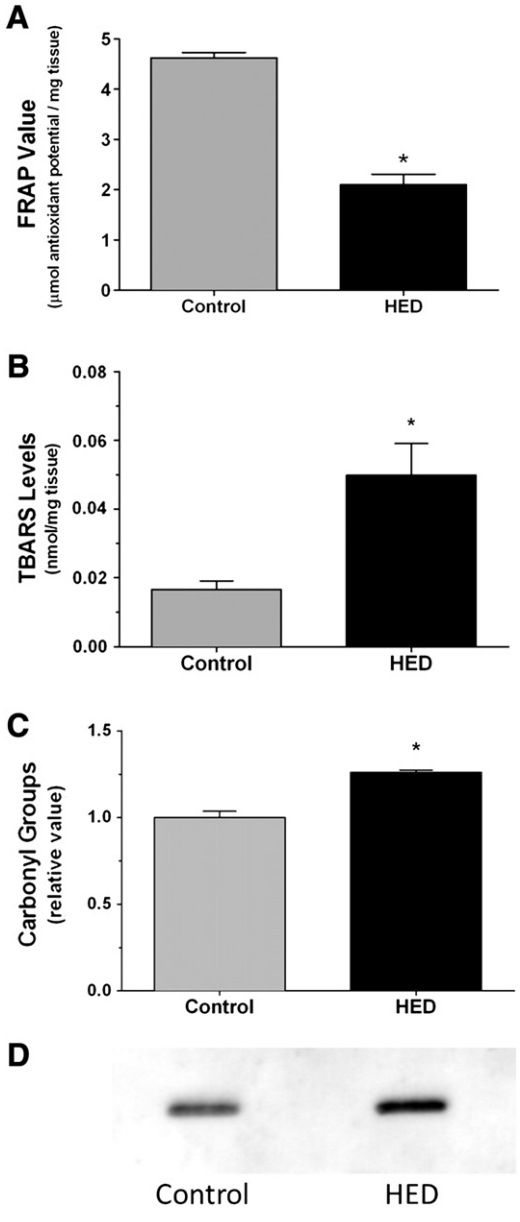

Fig. 5. A) Testicular antioxidant capacity in control group and HED group. B) Testicular lipid peroxidation in control group and HED group. C) Testicular carbonyl content in control group and HED group. D) Illustrative representation of carbonyl content by Slot Blot. Results are presented as mean ± SEM of five independent experiments, corresponding to five animals/group and performed in duplicate. *$P < 0.05$ vs. control group.

Testicles present high lipid content, which are known to be a major target of ROS. Increased testicular ROS activity may lead to lipid peroxidation, therefore we evaluated the TBARS content in testicular homogenates as a measure of lipid peroxidation. We observed a significant increase of testicular TBARS content from 0.0166 nmol/mg tissue (in control group) to 0.0498 nmol/mg tissue in HED group (Fig. 5B). These results demonstrate a 3-fold increase on testicular lipid peroxidation levels in testicles of HED-fed rats.

As it occurs for lipids, proteins are also sensitive to oxidation by ROS. The evaluation of protein carbonyl groups content has been widely used as biomarker of protein damage by oxidative stress [47]. As pre-diabetic animals presented an alteration on testicular antioxidant capacity, we evaluated the effect of pre-diabetes on testicular protein oxidation. Hence, animals from the HED group exhibited a 26% increase of testicular carbonyl content when compared to control group (Fig. 5C and D).

4. Discussion

Pre-diabetes is a pathological state that includes some (but not all) diagnostic criteria for DM [1], being characterized by IFG and/or IGT and by mild hyperglycemia [2]. In the present study, a HED-induced rodent model was used to evaluate the effects of this prodromal stage of DM in testicular PGC-1α/Sirt3 axis, as well as in mitochondrial bioenergetics and oxidative stress. As described by our team, this HED-fed rodent model displayed the characteristics of a pre-diabetic state as reported in other studies using the same animal model [14,26]. As expected, the HED fed animals developed mild hyperglycaemia and glucose intolerance, which are the two main characteristics of a pre-diabetic state. The mild hyperglycaemia observed in the HED animals did not meet the criteria for established DM [48]. However, those conditions together with the lower insulin levels, point toward a higher risk for DM [49,50]. The observed decrease in insulin levels may be caused by β-cell pancreatic failure. This hypothesis is supported by studies from Blazquez and Quijada [51], which observed hypoinsulinemia in high-fat fed animals. In fact, β-cells may present certain susceptibility to lipids [52], thus the dietary fats used in HED may induce β-pancreatic cell failure, decreasing insulin secretion. Furthermore, impaired insulin secretion has also been described in adolescents with pre-diabetes, particularly those with a higher BMI, presenting a higher risk for progression to T2DM [53].

The well-functioning of the PGC-1α/Sirt3 axis has been reported as essential for the regulation of mitochondrial metabolism, biogenesis and oxidative stress [16,54]. PGC-1α arises as a key regulator of mitochondrial function, since it co-activates several nuclear transcriptors, which in turn regulate the expression of nuclear encoded mitochondrial proteins. PGC-1α is also essential for the expression of Sirt3. Recently Kong and collaborators [16] showed that PGC-1α knockdown effectively reduces Sirt3 expression in muscle cells and hepatocytes, which regulates important mitochondrial functions by deacetylating several metabolic and respiratory enzymes [19,22]. Disturbances of PGC-1α levels have been linked to the development of DM [55]. Furthermore, it has also been reported that Sirt3 is decreased by high-fat consumption [56,57], as well as under diabetic conditions [24], which is concomitant with PGC-1α decrease [23].

In our work we identified the expression of PGC-1α and Sirt3 on the testicles of 3-month old Wistar rats. Importantly, we found that at testicular level both the PGC-1α and Sirt3 protein levels were significantly decreased on the animals of the HED group. This decrease in PGC-1α levels may be deleterious for testicular mitochondrial physiology, particularly because this effect can be exacerbated by downregulation of Sirt3. Our results suggest that the reduced expression of PGC-1α compromises the expression of Sirt3 in the testicles of HED-fed rats. Although, to the date, there are no direct reports demonstrating that down-regulation of PCG-1α leads to reduced SIRT3 levels within testicular *milieu*, Kong and collaborators recently described a molecular mechanism for Sirt3 expression, where PGC-1α functions as an

upstream activator of Sirt3 gene expression in muscle cells and hepatocytes, having a stimulatory effect on Sirt3 promoter [16]. The results obtained herein suggest that the reduced expression of PGC-1α compromises the expression mechanism of Sirt3, thus decreasing testicular Sirt3 content. So, in these conditions the expression of testicular Sirt3 may be downregulated at transcriptional level, leading to a decreased Sirt3 protein levels.

Decreased levels of PGC-1α and Sirt3 are known to modulate mitochondrial metabolic activity and oxidative stress regulatory pathway activation [19,56]. We have previously reported that the high glycolytic flux evidenced by HED animals favored an oxidative environment within testicles [14], which could compromise cellular integrity. In this context, PGC-1α is required to the induction of ROS-detoxifying enzymes under oxidative stress conditions [16], whereas PGC-1α knockdown blunts antioxidant capacity [58]. Recently Kong and collaborators [16] showed that PGC-1α acts as a ROS suppressor by increasing the expression of glutathione peroxidase 1 and superoxide dismutase 2 [54,59]. Additionally, it has also been reported that Sirt3 induces the expression of antioxidant defenses [60], thus mediating the effects of PGC-1α on ROS levels. This highlights the synergistic role between PGC-1α and Sirt3 in the control of the oxidative stress status [16]. Indeed, HED-fed rats presented a deficient testicular antioxidant capacity, which may result in part from the significant deregulation of the PGC-1α/Sirt3 axis, thus enhancing testicular ROS overproduction. Our results show an increased level of carbonyl content and TBARS in testicles of HED rats, evidencing a higher testicular susceptibility to oxidation associated with pre-diabetes. In fact the decreased levels of Sirt3 may contribute to this, since it has been reported that Sirt3 knockout animals present the highest levels of hepatic and neuronal lipid peroxidation and protein carbonylation [61].

Additionally, we observed a significant decrease in testicular mtDNA content in HED-fed rats, further evidencing that the pre-diabetic condition is deleterious for the mitochondrial function. The mtDNA content loss in this case is likely related to mitochondrial biogenesis, and PGC-1α is connected with the co-activation of several nuclear transcriptors such as NRF-1, NRF-2 and TFAM, directly involved in the signaling pathways that lead to mtDNA replication [62]. Despite that NRF-1, NRF-2 and TFAM are PGC-1α responsive genes, the unaltered levels of testicular NRF-1, NRF-2 and TFAM between HED-fed and control rats might involve compensatory mechanisms that are known to be triggered under oxidative stress conditions in order to maintain mitochondrial biogenesis as those described in hepatic oxidative conditions [63]. Furthermore, though protein levels were not altered, it is expectable that their activities are downregulated, since it has also been suggested that Sirt3 is capable of regulating the activities of NRF1 and TFAM, which localize in the mitochondria [16]. Additionally, mtDNA is also highly susceptible to oxidative stress, partly due to its localization. mtDNA is packaged into a protein-DNA complex known as a mitochondrial nucleoid, however due to the imbalance between ROS scavenging and overproduction, which is exacerbated by disruption of PGC-1α/Sirt3 axis, the composition of mtDNA nucleoid may be severely compromised thus contributing to mtDNA degradation within the testicular *milieu* of pre-diabetic rats. This is supported by the fact that PGC-1α and Sirt3 are essential for ROS-detoxifying system and downregulation of both proteins decrease the antioxidant defenses leading to compromised mtDNA integrity [23,64].

It has also been described that DM affects mitochondrial function by impairing ETC complexes enzymatic activities [65,66]. Although it has been reported that citrate synthase activity is diminished under diabetic conditions [65,67], we failed to observe significant differences on testicular citrate synthase activity in HED-fed rats, suggesting that testicular mitochondrial integrity may be unaltered. This may be explained by the fact that our animal model was in a prodromal stage of DM, not suffering the co-morbidities related with the later stages of the disease [68]. On the other hand, we found that HED fed rats presented a significant increase in testicular NADH reductase (complex I) activity. This observation is inconsistent with previous report, using a knockout model for Sirt3 that demonstrated reduced complex I activity [21]. Indeed, knockout models fail to show the molecular and cellular adaptations that might occur in wild type animals. Testicles are organs with high-energy demands and sperm are highly dependent on aerobic metabolism [69], so the increased mitochondrial complex I activity might be a compensatory mechanism by testicular mitochondria in response to metabolic changes caused by pre-diabetic state, in order to maintain a correct electron transport chain function and guarantee an adequate energy supply to the spermatogenic event. Furthermore, the observed increase in mitochondrial complex I activity in HED animals is consistent with the reported increase of mitochondrial oxidative capacity observed in other diet-induced animal models [70]. After NADH oxidation, the electrons flow sequentially through cytochrome c reductase (complex III), which funnels electrons from the coenzyme Q pool to cytochrome c [71]. The significant decrease observed in mitochondrial complex III activity of HED-fed rat testicles may be caused by the decreased levels of Sirt3, since complex III is one of the several main targets of this deacetylase protein [22]. The decoupling in complex I and complex III activities reverse the electron flow, favoring ROS production and impairing ATP synthesis, which could further exacerbate the pro-oxidative environment previously described in the testicles of HED rats by our team [14].

Disruption of PGC-1α/Sirt3 axis presented by pre-diabetic animals induces important changes in testicular ETC function, particularly at the level of complex I and complex III. The observed changes in ETC is a consequence of both PGC-1α and Sirt3 deregulation and whole testicular metabolic fluctuations [14], since testicles are compartmentalized organs presenting special metabolic characteristics and energy demands that confer a special microenvironment to testicular *milieu* [72–75]. Although it has been reported that DM can severely affect testicular ATP production [15], to our knowledge the testicular energetic status in pre-diabetic individuals remains undisclosed. The significant decrease in testicular ATP levels of HED-fed rats reported herein results from the disruption of PGC-1α/Sirt3 axis with a consequent impairment of ETC function. Moreover, such decrement in testicular ATP content may arise from its hydrolysis to subsequent adenine nucleotides (ADP and AMP) and adenosine metabolites. This hypothesis is further supported by the lower ADP levels we observed in HED-fed rats, suggesting that adenylate kinase reaction could be operating toward AMP production. Accordingly, testicular AMP levels were significantly increased in HED rats. Noteworthy, the imbalance in adenine nucleotides underlies a lower testicular ATP/AMP ratio, evidencing a decreased testicular AEC in HED rats. In these conditions, AMP may arise as a key regulatory molecule, enhancing catabolic pathways, such as glycolysis [76].

Regarding the hypoxanthine accumulation reported in testicles from HED rats, our previous work suggested that it could result from the high testicular glycolytic flux [14]. Indeed, high hypoxanthine levels have been correlated with an increased lactate/pyruvate ratio [77], which may also reflect the redox state of cells and tissues [78]. Altogether, our results show that HED-induced pre-diabetes downregulates both PGC-1α and Sirt3 protein expression, disrupting this axis with a consequent impairment on testicular mitochondrial bioenergetics (especially in complex I and complex III) and testicular AEC. It leads to hypoxanthine accumulation that may culminate in increased oxidative damage to testicular cells. Clearly, testicular function of HED animals is severely affected even in a prodromal stage of diabetes. Furthermore, this is strongly supported by previous observations by our team using this HED model [14,42], where we showed decreased testicular weight and compromised testicular function, including lower testicular testosterone content and altered sperm quality. To our knowledge, this is the first report giving new insights in the role of PGC-1α/Sirt3 axis in overall testicular bioenergetics at this prodromal "silencing stage" of DM. This topic should deserve special attention, as the subtle changes in testicular glucose metabolism and mitochondrial bioenergetics occurring earlier in the pathology may have a later severe negative impact in male fertility.

Funding

This work was supported by the Portuguese "Fundação para a Ciência e a Tecnologia"—FCT, co-funded by FEDER via Programa Operacional Factores de Competitividade—COMPETE/QREN (PTDC/QUI-BIQ/121446/2010 and PEst-C/SAU/UI0709/2011). L. Rato (SFRH/BD/72733/2010), A. I. Duarte (SFRH/BPD/26872/2006) and M. G. Alves (SFRH/BPD/80451/2011) were financed by FCT and European Social Fund. P. F. Oliveira was financed by FCT through FSE and POPH funds (Programa Ciência 2008).

Acknowledgements

The authors would like to thank Gonçalo Pereira, Sónia Correia, Renato Santos and António José Moreno for the assistance in ETC enzymatic protocols. The authors would also like to thank Gilberto Alves for the animal handling assistance.

References

[1] A.A.D., ADA, Diagnosis and classification of diabetes mellitus, Diabetes Care 35 (Suppl. 1) (2012) S64–S71.
[2] A.G. Tabák, C. Herder, W. Rathmann, E.J. Brunner, M. Kivimaki, Prediabetes: a high-risk state for diabetes development, Lancet 379 (2012) 2279–2290.
[3] W. Lutz, Fertility rates and future population trends: will Europe's birth rate recover or continue to decline? Int. J. Androl. 29 (2006) 25–33.
[4] E. D'Adamo, S. Caprio, Type 2 diabetes in youth: epidemiology and pathophysiology, Diabetes Care 34 (Suppl. 2) (2011) S161–S165.
[5] R. Weiss, S.E. Taksali, W.V. Tamborlane, T.S. Burgert, M. Savoye, S. Caprio, Predictors of changes in glucose tolerance status in obese youth, Diabetes Care 28 (2005) 902–909.
[6] N. Gungor, S. Arslanian, Progressive beta cell failure in type 2 diabetes mellitus of youth, J. Pediatr. 144 (2004) 656–659.
[7] A.L. Rosenbloom, J.R. Joe, R.S. Young, W.E. Winter, Emerging epidemic of type 2 diabetes in youth, Diabetes Care 22 (1999) 345–354.
[8] M. Delfino, N. Imbrogno, J. Elia, F. Capogreco, F. Mazzilli, Prevalence of diabetes mellitus in male partners of infertile couples, Minerva Urol. Nefrol. 59 (2007) 131–135.
[9] J.A. Attaman, T.L. Toth, J. Furtado, H. Campos, R. Hauser, J.E. Chavarro, Dietary fat and semen quality among men attending a fertility clinic, Hum. Reprod. 27 (2012) 1466–1474.
[10] T.K. Jensen, B.L. Heitmann, M.B. Jensen, T.I. Halldorsson, A.-M. Andersson, N.E. Skakkebaek, U.N. Joensen, M.P. Lauritsen, P. Christiansen, C. Dalgard, High dietary intake of saturated fat is associated with reduced semen quality among 701 young Danish men from the general population, Am. J. Clin. Nutr. 97 (2013) 411–418.
[11] M. Estienne, A. Harper, R. Crawford, Dietary supplementation with a source of omega-3 fatty acids increases sperm number and the duration of ejaculation in boars, Theriogenology 70 (2008) 70–76.
[12] R. Mitre, C. Cheminade, P. Allaume, P. Legrand, A.B. Legrand, Oral intake of shark liver oil modifies lipid composition and improves motility and velocity of boar sperm, Theriogenology 62 (2004) 1557–1566.
[13] M.G. Alves, A.D. Martins, L. Rato, P.I. Moreira, S. Socorro, P.F. Oliveira, Molecular mechanisms beyond glucose transport in diabetes-related male infertility, Biochim. Biophys. Acta 1832 (2013) 626–635.
[14] L. Rato, M.G. Alves, T.R. Dias, G. Lopes, J.E. Cavaco, S. Socorro, O.P.F., High-energy diets may induce a pre-diabetic state altering testicular glycolytic metabolic profile and male reproductive parameters, Andrology 1 (2013) 495–504.
[15] S. Amaral, A.J. Moreno, M.S. Santos, R. Seica, J. Ramalho-Santos, Effects of hyperglycemia on sperm and testicular cells of Goto-Kakizaki and streptozotocin-treated rat models for diabetes, Theriogenology 66 (2006) 2056–2067.
[16] X. Kong, R. Wang, Y. Xue, X. Liu, H. Zhang, Y. Chen, F. Fang, Y. Chang, Sirtuin 3, a new target of PGC-1α, plays an important role in the suppression of ROS and mitochondrial biogenesis, PLoS ONE 5 (2010) e11707.
[17] P. Puigserver, Z. Wu, C.W. Park, R. Graves, M. Wright, B.M. Spiegelman, A cold-inducible coactivator of nuclear receptors linked to adaptive thermogenesis, Cell 92 (1998) 829–839.
[18] Y. Shi, A. Dierckx, P.H. Wanrooij, S. Wanrooij, N.-G.r. Larsson, L.M. Wilhelmsson, M. Falkenberg, C.M. Gustafsson, Mammalian transcription factor A is a core component of the mitochondrial transcription machinery, Proc. Natl. Acad. Sci. 109 (2012) 16510–16515.
[19] T. Finkel, C.-X. Deng, R. Mostoslavsky, Recent progress in the biology and physiology of sirtuins, Nature 460 (2009) 587–591.
[20] E. Verdin, M.D. Hirschey, L.W. Finley, M.C. Haigis, Sirtuin regulation of mitochondria: energy production, apoptosis, and signaling, Trends Biochem. Sci. 35 (2010) 669–675.
[21] B.H. Ahn, H.S. Kim, S. Song, I.H. Lee, J. Liu, A. Vassilopoulos, C.X. Deng, T. Finkel, A role for the mitochondrial deacetylase Sirt3 in regulating energy homeostasis, Proc. Natl. Acad. Sci. 105 (2008) 14447–14452.
[22] L.W. Finley, A. Carracedo, J. Lee, A. Souza, A. Egia, J. Zhang, J. Teruya-Feldstein, P.I. Moreira, S.M. Cardoso, C.B. Clish, P.P. Pandolfi, M.C. Haigis, SIRT3 opposes reprogramming of cancer cell metabolism through HIF1alpha destabilization, Cancer Cell 19 (2011) 416–428.
[23] L.M. Sparks, H. Xie, R.A. Koza, R. Mynatt, M.W. Hulver, G.A. Bray, S.R. Smith, A high-fat diet coordinately downregulates genes required for mitochondrial oxidative phosphorylation in skeletal muscle, Diabetes 54 (2005) 1926–1933.
[24] E. Jing, B. Emanuelli, M.D. Hirschey, J. Boucher, K.Y. Lee, D. Lombard, E.M. Verdin, C.R. Kahn, Sirtuin-3 (Sirt3) regulates skeletal muscle metabolism and insulin signaling via altered mitochondrial oxidation and reactive oxygen species production, Proc. Natl. Acad. Sci. 108 (2011) 14608–14613.
[25] S. Amaral, P.J. Oliveira, J. Ramalho-Santos, Diabetes and the impairment of reproductive function: possible role of mitochondria and reactive oxygen species, Curr. Diabetes Rev. 4 (2008) 46–54.
[26] J. Ai, N. Wang, M. Yang, Z.M. Du, Y.C. Zhang, B.F. Yang, Development of Wistar rat model of insulin resistance, World J. Gastroenterol. 11 (2005) 3675–3679.
[27] Y. Zou, J. Li, C. Lu, J. Wang, J. Ge, Y. Huang, L. Zhang, Y. Wang, High-fat emulsion-induced rat model of nonalcoholic steatohepatitis, Life Sci. 79 (2006) 1100.
[28] S. Sivabalan, S. Renuka, V.P. Menon, Fat feeding potentiates the diabetogenic effect of dexamethasone in Wistar rats, Int. Arch. Med. 1 (2008) 7.
[29] V.L. Simões, M.G. Alves, A.D. Martins, T.R. Dias, L. Rato, S. Socorro, P.F. Oliveira, Regulation of apoptotic signaling pathways by 5α-dihydrotestosterone and 17β-estradiol in immature rat Sertoli cells, J. Steroid Biochem. Mol. Biol. 135 (2013) 15–23.
[30] T. Wai, A. Ao, X. Zhang, D. Cyr, D. Dufort, E.A. Shoubridge, The role of mitochondrial DNA copy number in mammalian fertility, Biol. Reprod. 83 (2010) 52–62.
[31] H.G. Coore, R.M. Denton, B.R. Martin, P.J. Randle, Regulation of adipose tissue pyruvate dehydrogenase by insulin and other hormones, Biochem. J. 125 (1971) 115–127.
[32] J. Long, J. Ma, C. Luo, X. Mo, L. Sun, W. Zang, J. Liu, Comparison of two methods for assaying complex I activity in mitochondria isolated from rat liver, brain and heart, Life Sci. 85 (2009) 276–280.
[33] H. Tisdale, Preparation and properties of succinic-cytochrome c reductase (complex II–III), Methods Enzymol. 10 (1967) 213–215.
[34] C. Luo, J. Long, J. Liu, An improved spectrophotometric method for a more specific and accurate assay of mitochondrial complex III activity, Clin. Chim. Acta 395 (2008) 38–41.
[35] D.L. Brautigan, S. Ferguson-Miller, E. Margoliash, Mitochondrial cytochrome c: preparation and activity of native and chemically modified cytochromes c, Methods Enzymol. 53 (1978) 128–164.
[36] A.C. Rego, M.S. Santos, C.R. Oliveira, Adenosine triphosphate degradation products after oxidative stress and metabolic dysfunction in cultured retinal cells, J. Neurochem. 69 (1997) 1228–1235.
[37] V. Stocchi, L. Cucchiarini, M. Magnani, L. Chiarantini, P. Palma, G. Crescentini, Simultaneous extraction and reverse-phase high-performance liquid chromatographic determination of adenine and pyridine nucleotides in human red blood cells, Anal. Biochem. 146 (1985) 118–124.
[38] I.F. Benzie, J. Strain, The ferric reducing ability of plasma (FRAP) as a measure of antioxidant power: the FRAP assay, Anal. Biochem. 239 (1996) 70–76.
[39] H. Ohkawa, N. Ohishi, K. Yagi, Assay for lipid peroxides in animal tissues by thiobarbituric acid reaction, Anal. Biochem. 95 (1979) 351–358.
[40] M. Iqbal, S. Sharma, H. Rezazadeh, N. Hasan, M. Abdulla, M. Athar, Glutathione metabolizing enzymes and oxidative stress in ferric nitilotriacetate mediated hepatic-injury, Redox Rep. 2 (1996) 385–391.
[41] R.L. Levine, D. Garland, C.N. Oliver, A. Amici, I. Climent, A.G. Lenz, B.W. Ahn, S. Shaltiel, E.R. Stadtman, Determination of carbonyl content in oxidatively modified proteins, Methods Enzymol. 186 (1990) 464–478.
[42] R.L. Bernardino, A.D. Martins, S. Socorro, M.G. Alves, P.F. Oliveira, Effect of prediabetes on membrane bicarbonate transporters in testis and epididymis, J. Membr. Biol. 246 (2013) 877–883.
[43] H.C. Lee, Y.H. Wei, Oxidative stress, mitochondrial DNA mutation, and apoptosis in aging, Exp. Biol. Med. (Maywood) 232 (2007) 592–606.
[44] R. Robinson, I.B. Fritz, Metabolism of glucose by Sertoli cells in culture, Biol. Reprod. 24 (1981) 1032–1041.
[45] F. Boussouar, M. Benahmed, Lactate and energy metabolism in male germ cells, Trends Endocrinol. Metab. 15 (2004) 345–350.
[46] T.V. Dunwiddie, L. Diao, W.R. Proctor, Adenine nucleotides undergo rapid, quantitative conversion to adenosine in the extracellular space in rat hippocampus, J. Neurosci. 17 (1997) 7673–7682.
[47] I. Dalle-Donne, R. Rossi, D. Giustarini, A. Milzani, R. Colombo, Protein carbonyl groups as biomarkers of oxidative stress, Clin. Chim. Acta 329 (2003) 23–38.
[48] Y.K. Sinzato, P.H. Lima, K.E. Campos, A.C. Kiss, M.V. Rudge, D.C. Damasceno, Neonatally-induced diabetes: lipid profile outcomes and oxidative stress status in adult rats, Rev. Assoc. Med. Bras. 55 (2009) 384–388.
[49] S. Andrikopoulos, A.R. Blair, N. Deluca, B.C. Fam, J. Proietto, Evaluating the glucose tolerance test in mice, Am. J. Physiol. Endocrinol. Metab. 295 (2008) E1323–E1332.
[50] S. Gupte, N. Labinskyy, R. Gupte, A. Csiszar, Z. Ungvari, J.G. Edwards, Role of NAD(P)H oxidase in superoxide generation and endothelial dysfunction in Goto-Kakizaki (GK) rats as a model of nonobese NIDDM, PLoS ONE 5 (2010) e11800.
[51] E. Blazquez, C.L. Quijada, The effect of a high-fat diet on glucose, insulin sensitivity and plasma insulin in rats, J. Endocrinol. 42 (1968) 489–494.
[52] C. Tang, A.E. Naassan, A. Chamson-Reig, K. Koulajian, T.T. Goh, F. Yoon, A.I. Oprescu, H. Ghanim, G.F. Lewis, P. Dandona, Susceptibility to fatty acid-induced β-cell dysfunction is enhanced in prediabetic diabetes-prone biobreeding rats: a potential

link between β-cell lipotoxicity and islet inflammation, Endocrinology 154 (2013) 89–101.
[53] F. Bacha, S. Lee, N. Gungor, S.A. Arslanian, From pre-diabetes to type 2 diabetes in obese youth pathophysiological characteristics along the spectrum of glucose dysregulation, Diabetes Care 33 (2010) 2225–2231.
[54] E.L. Bell, L. Guarente, The SirT3 divining rod points to oxidative stress, Mol. Cell 42 (2011) 561–568.
[55] A.M. Joseph, D.R. Joanisse, R.G. Baillot, D.A. Hood, Mitochondrial dysregulation in the pathogenesis of diabetes: potential for mitochondrial biogenesis-mediated interventions, Exp. Diabetes Res. (2012) 642038.
[56] M.D. Hirschey, T. Shimazu, E. Jing, C.A. Grueter, A.M. Collins, B. Aouizerat, A. Stancakova, E. Goetzman, M.M. Lam, B. Schwer, R.D. Stevens, M.J. Muehlbauer, S. Kakar, N.M. Bass, J. Kuusisto, M. Laakso, F.W. Alt, C.B. Newgard, R.V. Farese Jr., C.R. Kahn, E. Verdin, SIRT3 deficiency and mitochondrial protein hyperacetylation accelerate the development of the metabolic syndrome, Mol. Cell 44 (2011) 177–190.
[57] J. Bao, I. Scott, Z. Lu, L. Pang, C.C. Dimond, D. Gius, M.N. Sack, SIRT3 is regulated by nutrient excess and modulates hepatic susceptibility to lipotoxicity, Free Radic. Biol. Med. 49 (2010) 1230–1237.
[58] D. Marmolino, M. Manto, F. Acquaviva, P. Vergara, A. Ravella, A. Monticelli, M. Pandolfo, PGC-1alpha down-regulation affects the antioxidant response in Friedreich's ataxia, PLoS ONE 5 (2010) e10025.
[59] X. Qiu, K. Brown, M.D. Hirschey, E. Verdin, D. Chen, Calorie restriction reduces oxidative stress by SIRT3-mediated SOD2 activation, Cell Metab. 12 (2010) 662–667.
[60] N.R. Sundaresan, M. Gupta, G. Kim, S.B. Rajamohan, A. Isbatan, M.P. Gupta, Sirt3 blocks the cardiac hypertrophic response by augmenting Foxo3a-dependent antioxidant defense mechanisms in mice, J. Clin. Invest. 119 (2009) 2758–2771.
[61] S. Someya, W. Yu, W.C. Hallows, J. Xu, J.M. Vann, C. Leeuwenburgh, M. Tanokura, J.M. Denu, T.A. Prolla, Sirt3 mediates reduction of oxidative damage and prevention of age-related hearing loss under caloric restriction, Cell 143 (2010) 802–812.
[62] H.-C. Lee, Y.-H. Wei, Mitochondrial biogenesis and mitochondrial DNA maintenance of mammalian cells under oxidative stress, Int. J. Biochem. Cell Biol. 37 (2005) 822–834.
[63] H.B. Suliman, M.S. Carraway, K.E. Welty-Wolf, A.R. Whorton, C.A. Piantadosi, Lipopolysaccharide stimulates mitochondrial biogenesis via activation of nuclear respiratory factor-1, J. Biol. Chem. 278 (2003) 41510–41518.
[64] H. Kim, K. Patel, K. Muldoon-Jacobs, K.S. Bisht, N. Aykin-Burns, J.D. Pennington, R. van der Meer, P. Nguyen, J. Savage, K.M. Owens, SIRT3 is a mitochondria-localized tumor suppressor required for maintenance of mitochondrial integrity and metabolism during stress, Cancer Cell 17 (2010) 41–52.
[65] S.K. Chowdhury, E. Zherebitskaya, D.R. Smith, E. Akude, S. Chattopadhyay, C.G. Jolivalt, N.A. Calcutt, P. Fernyhough, Mitochondrial respiratory chain dysfunction in dorsal root ganglia of streptozotocin-induced diabetic rats and its correction by insulin treatment, Diabetes 59 (2010) 1082–1091.
[66] F.M. Ferreira, C.M. Palmeira, R. Seica, A.J. Moreno, M.S. Santos, Diabetes and mitochondrial bioenergetics: alterations with age, J. Biochem. Mol. Toxicol. 17 (2003) 214–222.
[67] A.P. Gomes, F.V. Duarte, P. Nunes, B.P. Hubbard, J.S. Teodoro, A.T. Varela, J.G. Jones, D.A. Sinclair, C.M. Palmeira, A.P. Rolo, Berberine protects against high fat diet-induced dysfunction in muscle mitochondria by inducing SIRT1-dependent mitochondrial biogenesis, Biochim. Biophys. Acta 1822 (2012) 185–195.
[68] K.E. Shortreed, M.P. Krause, J.H. Huang, D. Dhanani, J. Moradi, R.B. Ceddia, T.J. Hawke, Muscle-specific adaptations, impaired oxidative capacity and maintenance of contractile function characterize diet-induced obese mouse skeletal muscle, PLoS ONE 4 (2009) e7293.
[69] M. Bajpai, G. Gupta, B. Setty, Changes in carbohydrate metabolism of testicular germ cells during meiosis in the rat, Eur. J. Endocrinol. 138 (1998) 322–327.
[70] E. Chanseaume, A.L. Tardy, J. Salles, C. Giraudet, P. Rousset, A. Tissandier, Y. Boirie, B. Morio, Chronological approach of diet-induced alterations in muscle mitochondrial functions in rats, Obesity (Silver Spring) 15 (2007) 50–59.
[71] P. Kakkar, B.K. Singh, Mitochondria: a hub of redox activities and cellular distress control, Mol. Cell. Biochem. 305 (2007) 235–253.
[72] P.F. Oliveira, M.G. Alves, L. Rato, S. Laurentino, J. Silva, R. Sa, A. Barros, M. Sousa, R.A. Carvalho, J.E. Cavaco, S. Socorro, Effect of insulin deprivation on metabolism and metabolism-associated gene transcript levels of in vitro cultured human Sertoli cells, Biochim. Biophys. Acta 1820 (2012) 84–89.
[73] M.G. Alves, L. Rato, R.A. Carvalho, P.I. Moreira, S. Socorro, P.F. Oliveira, Hormonal control of Sertoli cell metabolism regulates spermatogenesis, Cell. Mol. Life Sci. 70 (2013) 777–793.
[74] L. Rato, M. Alves, S. Socorro, R.A. Carvalho, J.E. Cavaco, P.F. Oliveira, Metabolic modulation induced by oestradiol and DHT in immature rat Sertoli cells cultured in vitro, Biosci. Rep. 32 (2012) 61–69.
[75] L. Rato, M.G. Alves, S. Socorro, A.I. Duarte, J.E. Cavaco, P.F. Oliveira, Metabolic regulation is important for spermatogenesis, Nat. Rev. Urol. 9 (2012) 330–338.
[76] D.G. Hardie, S.A. Hawley, AMP-activated protein kinase: the energy charge hypothesis revisited, Bioessays 23 (2001) 1112–1119.
[77] P.N. Bjerring, J. Hauerberg, L. Jorgensen, H.J. Frederiksen, F. Tofteng, B.A. Hansen, F.S. Larsen, Brain hypoxanthine concentration correlates to lactate/pyruvate ratio but not intracranial pressure in patients with acute liver failure, J. Hepatol. 53 (2010) 1054–1058.
[78] J.M. O'Donnell, R.K. Kudej, K.F. LaNoue, S.F. Vatner, E.D. Lewandowski, Limited transfer of cytosolic NADH into mitochondria at high cardiac workload, Am. J. Physiol. Heart Circ. Physiol. 286 (2004) H2237–H2242.